faces on cooling (Datars, van Schyndel, Lass, Chartier & Gillespie, 1978).

The r.m.s. atomic displacement parameters (U) of the F atoms show a large anisotropy. In particular, $U_{22} \gg U_{11}$ for $F(1)$ and $U_{33} > U_{11}$ for F(2) in all the room-temperature structures. This feature was attributed by Tun & Brown (1982) to an artifact of a static rotational disorder of the MF_6 ion induced by the variable position of the Hg atoms in the adjacent chain. Since the chains and the host lattice remain incommensurate even at $T < T_c$, only a small change in U_{22} of F(1) and U_{33} of F(2) with temperature was then expected. However, the large ratios of displacement parameters observed [$\langle U(173\text{ K})/U(293\text{ K})\rangle = 0{\cdot}50$ for $Hg_{3-\delta}SbF_6$ and $\langle U(150\text{ K})/U(293\text{ K})\rangle = 0{\cdot}43$ for $Hg_{3-\delta}TaF_6$] are roughly proportional to the ratios of the temperatures of measurement (0·59 and 0·51 respectively) suggesting that the anisotropies in the r.m.s. displacements of the F atoms at room temperature are dynamic and presumably are coupled to the thermal sliding modes of the chains.

The competition between parallel and perpendicular coupling

The L phase is produced by a direct repulsion between the atoms in neighbouring perpendicular chains and results in a structure in which the Hg atoms avoid each other at the crossing points. The distance between chains is about 3·24 Å (at 293 K) in all three structures, $Hg_{3-\delta}AsF_6$, $Hg_{3-\delta}SbF_6$ and $Hg_{3-\delta}TaF_6$, so that the strength of the interaction is probably similar and results in the distance between nearest-neighbour Hg atoms in perpendicular chains ranging between 3·34 and 3·47 Å. On the other hand, the interaction between parallel chains which is mediated by the host lattice will change as the anion becomes larger. The effect of this can be seen in the poorer ordering in the S phase of the Sb and Ta compounds compared to As and the higher temperature at which the transition to the L phase occurs.

We wish to thank the Natural Sciences and Engineering Research Council of Canada for an operating grant and Brookhaven National Laboratory for assistance in the measurement of T_c for $Hg_{3-\delta}SbF_6$.

References

AXE, J. D. (1980). In *Ordering in Strongly Fluctuating Condensed Matter Systems*, edited by T. RISTE. New York: Plenum.

BROWN, I. D., CUTFORTH, B. D., DAVIES, C. G., GILLESPIE, R. J., IRELAND, P. R. & VEKRIS, J. E. (1974). *Can. J. Chem.* **52**, 791-793.

DATARS, W. R., VAN SCHYNDEL, A., LASS, J. S., CHARTIER, D. & GILLESPIE, R. J. (1978). *Phys. Rev. Lett.* **40**, 1184-1187.

EMERY, V. J. & AXE, J. D. (1978). *Phys. Rev. Lett.* **40**, 1507-1511.

HASTINGS, J. M., POUGET, J. P., SHIRANE, G., HEEGER, A. J., MIRO, N. D. & MACDIARMID, A. G. (1977). *Phys. Rev. Lett.* **39**, 1484-1487.

KHAN, A. A. (1976). *Acta Cryst.* A**32**, 11-16.

LARSON, A. C. (1967). *Acta Cryst.* **23**, 664-665.

POUGET, J. P., SHIRANE, G., HASTINGS, J. M., HEEGER, A. J., MIRO, N. D. & MACDIARMID, A. G. (1978). *Phys. Rev. B*, **18**, 3645-3656.

SPAL, R., CHEN, C. E., EGAMI, T., NIGREY, P. J. & HEEGER, A. J. (1980). *Phys. Rev. B*, **21**, 3110-3118.

TUN, Z. (1985*a*). PhD thesis (Appendix), McMaster Univ., Hamilton, Ontario, Canada L8S 4M1.

TUN, Z. (1985*b*). PhD thesis, Table 1, available from the Thode Library, McMaster Univ., Hamilton, Ontario, Canada L8S 4M1.

TUN, Z. & BROWN, I. D. (1982). *Acta Cryst.* B**38**, 2321-2324.

TUN, Z., BROWN, I. D. & UMMAT, P. K. (1984). *Acta Cryst.* C**40**, 1301-1303.

Acta Cryst. (1986). B**42**, 213-224

On the Prediction of Structure Changes in Bi_2O_3 Caused by Ordering and Pseudo-Jahn–Teller Instability

BY KARIN KHACHATURYAN

Nov. Cheremushka 32*a*, *Bl5-Apt* 40, *Moscow* 113461, *USSR*

(*Received* 22 *July* 1985: *accepted* 14 *August* 1985)

Abstract

The structures of the β and δ phases of Bi_2O_3 are predicted theoretically. The concentration-wave method is used to determine the oxygen ordering over tetrahedral interstices of the f.c.c. Bi host. This method yields two modifications for the δ phase. One is a disordered phase in which O atoms randomly occupy tetrahedral interstices of the f.c.c. host. This structure agrees with the model proposed by Gattow & Schröder [*Z. Anorg. Allg. Chem.* (1962), **318**, 176-189]. The second modification is the interstitial superstructure in which O atoms are regularly distributed over tetrahedral sites. Its structure agrees with the Sillen model [Sillen (1937). *Ark Kemi Mineral. Geol.* **12A**, 1-15]. It is shown that the structure of the β

0108-7681/86/030213-12$01.50

phase cannot be obtained as a result of oxygen ordering only, but is formed by a combination of ordering and two successive displacive transformations. It is shown that these displacive transformations can be explained by the pseudo-Jahn–Teller effect. The second displacive transformation occurs only for the non-stoichiometric β phase. The final structure of the β phase agrees with that obtained by X-ray diffraction.

Introduction

As has been shown before (Khachaturyan & Pokrovskii, 1985), many oxides of transition and non-transition metals may be regarded as interstitial superstructures in which atoms of one sort are distributed in an ordered manner over the interstices of a host structure formed by atoms of the other sort. In this case, the crystal-structure-determination problem can be formulated within the framework of the Ising model, which thus enables one to employ modern developments in the statistical mechanics of ordered alloys, particularly the method of static concentration waves (Khachaturyan, 1962, 1963, 1973, 1978; Khachaturyan & Pokrovskii, 1985), to determine the atomic structure of a stable oxide from simple interatomic interaction models. Application of the Ising model does not necessarily require the rigid-lattice approximation. Atomic displacements generated by an ordered distribution of atoms (such displacements, of course, are unable to change the symmetry of the ordered phase) can be easily included in the Ising model without any significant complications. The consideration of such displacements merely leads to a strain-induced contribution to the pairwise interatomic energies. This is, however, not the case with any non-trivial displacements that reduce the symmetry of a crystal with respect to the symmetry imposed by the ordered atomic distribution. The amplitudes of such displacive modes can be regarded as the long-range-order parameters of the system. They characterize a diffusionless phase transformation that is quite a common phenomenon in crystals. Therefore, the prediction of the atomic structure of some crystals cannot be successfully carried out if additional displacive long-range-order parameters are ignored. An example of the theoretical prediction of an atomic structure is presented below for the particular case of the Bi_2O_3 oxides. In this example, both effects, ordering and spontaneous displacements, are taken into account. It is shown that spontaneous displacements in β-Bi_2O_3 are caused by the pseudo-Jahn–Teller transition.

Some Bi_2O_3 oxides can be regarded as interstitial superstructures in which oxygen atoms are ordered over tetrahedral interstices of the f.c.c. host structure formed by bismuth atoms. Before proceeding to further discussions it is worth recalling the main results of the concentration-wave approach (Khachaturyan, 1962, 1978), as applied to this specific case, *viz* the f.c.c. host structure with tetrahedral site occupancy.

1. Concentration-wave method results for interstitial superlattices based on the f.c.c. host structure

Each site of the f.c.c. host structure has two nearest-neighbour tetrahedral interstices, T_1 and T_2, which are displaced from the nearest host site by the vectors

$$\mathbf{h}_1 = \tfrac{1}{4}(\mathbf{a}_1+\mathbf{a}_2+\mathbf{a}_3); \quad \mathbf{h}_2 = -(\mathbf{a}_1+\mathbf{a}_2+\mathbf{a}_3), \qquad (1)$$

where $\mathbf{a}_1$, $\mathbf{a}_2$, $\mathbf{a}_3$ are the f.c.c. lattice translations along the [100], [010], [001] axes, respectively. Translation of the host site and the two tetrahedral sites generates f.c.c. host sites and the two f.c.c. sublattices T_1 and T_2 of tetrahedral sites, respectively.

If O atoms occupy all of the tetrahedral sites, the fluorite structure will arise. If O atoms occupy only some of the tetrahedral sites, the system acquires configurational degrees of freedom associated with the possibility of redistribution of O atoms. In this case the pairwise O–O interaction energy is

$$U = \tfrac{1}{2}\sum_{p,q}\sum_{\mathbf{R},\mathbf{R}'} W_{pq}(\mathbf{R}-\mathbf{R}')c(p,\mathbf{R})c(q,\mathbf{R}'), \qquad (2)$$

where $\mathbf{R}$ and $\mathbf{R}'$ label f.c.c. host sites, $(p, \mathbf{R})$ and $(q, \mathbf{R}')$ are the 'addresses' of tetrahedral sites nearest to the host sites $\mathbf{R}$ and $\mathbf{R}'$, respectively (by definition p, $q = 1, 2$), $W_{pq}(\mathbf{R}-\mathbf{R}')$ is the energy of pairwise interaction of two O atoms at the tetrahedral sites $(p, \mathbf{R})$ and $(q, \mathbf{R}')$, and $c(p, \mathbf{R})$ is an occupation number equal to unity if the site $(p, \mathbf{R})$ is occupied by an O ion and zero otherwise.

The distribution of O atoms is determined by the occupation probabilities

$$n(p,\mathbf{R}) = \langle c(p,\mathbf{R})\rangle, \qquad (3)$$

where $\langle\cdots\rangle$ denotes averaging over the canonical ensemble. At high temperatures substantially exceeding typical O–O interaction energies the equilibrium distribution is

$$n(p,\mathbf{R}) = c = \text{constant},$$

where c is the O:2Bi ratio, *i.e.* all interstitial sites are occupied with the same probability c. This distribution describes the homogeneous disordered state. Below the order–disorder transition temperature T_0, the occupation probabilities $n(p, \mathbf{R})$ become dependent on interstitial site coordinates $(p, \mathbf{R})$ and thus describe the atomic structure of the ordered phase.

Interaction energy (2) is a quadratic form of the occupation numbers $c(p, \mathbf{R})$. The diagonal representation of the quadratic form (2) is determined

by the eigenvalues and eigenvectors of the matrix

$$V_{pq}(\mathbf{k}) = \sum_{\mathbf{R}} W_{pq}(\mathbf{R}) \exp(-i2\pi\mathbf{kR}) = \begin{pmatrix} V_{11}(\mathbf{k}) & V_{12}(\mathbf{k}) \\ V_{12}(\mathbf{k})^* & V_{11}(\mathbf{k}) \end{pmatrix}. \quad (4)$$

Eigenvalues of matrix (4) form two branches of the spectrum

$$\lambda_{(\pm)} = V_{11}(\mathbf{k}) \pm |V_{12}(\mathbf{k})|. \quad (5)$$

The corresponding eigenvectors are

$$v_{(\pm)}(p, \mathbf{k}) = 2^{-1/2}[1, \pm V_{12}(\mathbf{k})^*/|V_{12}(\mathbf{k})|]. \quad (6)$$

According to the concentration-wave method, a decrease in temperature results in the instability of a disordered homogeneous system against static concentration waves

$$v_{(-)}(p, \mathbf{k}_{0j}) \exp(i2\pi\mathbf{k}_{0j}\mathbf{R}) \quad (7)$$

corresponding to the minimal eigenvalue of matrix (4)

$$\lambda_{(-)}(\mathbf{k}_{0j}) = \min \lambda_{(\pm)}(\mathbf{k}) = \min \lambda_{(-)}(\mathbf{k}), \quad (8)$$

where $\mathbf{k}_{0j}$ are vectors of the star minimizing the function $\lambda_{(-)}(\mathbf{k})$ (the star is a set of wavevectors $\mathbf{k}_{0j}$ that may be obtained from one wavevector by applying to it all operations of the symmetry group of the disordered solution). It is assumed that the vectors $\mathbf{k}_{0j}$, differing from each other by a fundamental reciprocal-lattice vector are identical.

Such an instability leads to the onset of an ordered state. The temperature of the order-disorder transition in the mean field approximation is given by (Khachaturyan, 1963)

$$T_0 = -[c(1-c)/k_B] \min \lambda_{(\pm)}(\mathbf{k}) = -[c(1-c)/k_B]\lambda_{(-)}(\mathbf{k}_{0j}), \quad (9)$$

where k_B is the Boltzmann constant. The ordered distribution of interstitial atoms may then be described by the superposition of the concentration waves (7):

$$n(p, \mathbf{R}) = c + \eta \sum_j \gamma_{(-)}(\mathbf{k}_{0j}) v_{(-)}(p, \mathbf{k}_{0j}) \times \exp(i2\pi\mathbf{k}_{0j}\mathbf{R}), \quad (10)$$

where η is the long-range parameter and the coefficients $\gamma_{(-)}(\mathbf{k}_{0j})$ are chosen to meet the following two conditions:

(i) the number of different values of $n(p, \mathbf{R})$ on all crystal sites $(p, \mathbf{R})$ of the ordered phase should be greater by unity than the total number of long-range-order parameters in the expression for $n(p, \mathbf{R})$. In the case (10) when the sole long-range-order parameter is contained in the expression for $n(p, \mathbf{R})$, $n(p, \mathbf{R})$ should assume only two values on all sites $(p, \mathbf{R})$;

(ii) $n(p, \mathbf{R})$ should be equal to unity or zero for all long-range-order parameters equal to unity.

The condition (ii) also determines stoichiometric composition $c = c_{st}$ of the compound described by (10). In practice, the value of c_{st} is determined by the valency of the compound and is known in advance. The valency of the compound thus imposes constraints on the choice of value of coefficients $\gamma_{(-)}(\mathbf{k}_{0j})$. Each tetrahedral interstice T_1 has six nearest T_2 interstices separated from it by the vectors $\{\frac{1}{2}a, 0, 0\}$, 12 next-nearest T_1 interstices and eight T_2 interstices, separated from the reference interstice by the vectors $\{\frac{1}{2}a, \frac{1}{2}a, 0\}$ and $\{\frac{1}{2}a, \frac{1}{2}a, \frac{1}{2}a\}$, respectively. The corresponding interaction energies are W_1, W_2 and W_3, respectively. With the approximation that the interaction is non-zero only for three coordination shells then

$$\begin{aligned} V_{11}(\mathbf{k}) &= 4W_2(\cos\pi k_x \cos\pi k_y + \cos\pi k_x \cos\pi k_z + \cos\pi k_y \cos\pi k_z) \\ V_{12}(\mathbf{k}) &= \exp[i\pi(k_x + k_y + k_z)][2W_1(\cos\pi k_x + \cos\pi k_y + \cos\pi k_z) \\ &\quad + 8W_3 \cos\pi k_x \cos\pi k_y \cos\pi k_z], \end{aligned} \quad (11)$$

where $\mathbf{k} = a^{-1}(k_x, k_y, k_z)$; k_x, k_y, k_z are coordinates along the [100], [010], [001] directions. Substitution of (11) in (5) and (6) yields for the lower branch

$$\begin{aligned} \lambda_{(-)}(\mathbf{k}) &= 4W_2(\cos\pi k_x \cos\pi k_y + \cos\pi k_x \cos\pi k_z + \cos\pi k_y \cos\pi k_z) \\ &\quad - |2W_1(\cos\pi k_x + \cos\pi k_y + \cos\pi k_x) \\ &\quad + 8W_3 \cos\pi k_x \cos\pi k_y \cos\pi k_z|. \end{aligned} \quad (12)$$

The corresponding eigenvector is

$$\begin{aligned} v_{(-)}(p, \mathbf{k}) = 2^{-1/2}\{1 - [\, &W_1(\cos\pi k_x + \cos\pi k_y + \cos\pi k_z) \\ &+ 4W_3(\cos\pi k_x \cos\pi k_y \cos\pi_z)] \\ &\times |W_1(\cos\pi k_x + \cos\pi k_y + \cos\pi k_z) \\ &+ 4W_3(\cos\pi k_x \cos\pi k_y \cos\pi k_z)|^{-1} \\ &\times \exp[-i\pi(k_x + k_y + k_y + k_z)]\}. \end{aligned} \quad (13)$$

2. Phase transformations in Bi_2O_3

As mentioned above, bismuth oxides may be conveniently described as interstitial superstructures formed by O atoms occupying tetrahedral interstices of the f.c.c. array formed by the Bi atoms. The stoichiometric composition of the oxides is determined by the valences of oxygen and bismuth and is equal to $c_{st} = O/2Bi = 3/4$. This means that 3/4 of the tetrahedral interstices are occupied by oxygen atoms. If the possibility of displacive transformations is ignored in the first approximation, the structures of

the various phases of Bi_2O_3 may be described in terms of ordering of O atoms and their vacancies over tetrahedral interstices.

(*a*) At temperatures higher than the T_0 of (9), oxygen atoms are randomly distributed over the interstices and $n(p, \mathbf{R}) = c_{st} = 3/4$. The corresponding high-temperature phase (if it exists below the melting temperature) should have the non-stoichiometric structure of fluorite.

(*b*) In order to determine the structure of Bi_2O_3 characterized by an ordered distribution of oxygen vacancies, one should find, according to the procedure described in the *Introduction*, the wavevector $\mathbf{k}_{0j}$ and the eigenvector $v_{(-)}(p, \mathbf{k}_{0j})$ providing the minimum of $\lambda_{(-)}(\mathbf{k})$.

The natural assumption that O^{2-} ions bearing the same charge repel each other and that repulsion energies decrease with distance yields

$$W_1 > W_2 > W_3 > 0.$$

Analysis of spectrum (12) at various values of the parameters W_1, W_2 and W_3 shows that the minimum values of $\lambda_{(-)}(\mathbf{k})$ are attained at $\mathbf{k} = 0$ and at the vectors of the star $\mathbf{k} = \{100\}$. It follows from (13) that at $\mathbf{k} = 0$

$$v_{(-)}(p, 0) = 2^{-1/2}(1, -1), \tag{14}$$

i.e. the disordered state is unstable against onset of the ordered distribution (10). Substitution of (14) into (10) yields

$$n(p, \mathbf{R}) = c + \eta\gamma_{(-)}(0)v_{(-)}(p, 0) = \begin{cases} c + \eta\gamma_{(-)}(0)2^{-1/2} \\ c - \eta\gamma_{(-)}(0)2^{-1/2}. \end{cases} \tag{15}$$

Distribution (15) assumes two values 0 and 1 for $\eta = 1$ provided that $\gamma_{(-)}(0) = 2^{-1/2}$, $c = c_{st} = \frac{1}{2}$. The corresponding distribution describing the ZnS-type structure does not meet the condition $c_{st} = \frac{3}{4}$ and should therefore be rejected. It follows from (12) and (13) that

(i) if $W_3/W_1 < \frac{1}{4}$,

$$v_{(-)}(p, \mathbf{k}_{0j}) = 2^{-1/2}(1, 1) \tag{16a}$$

(ii) if $W_3/W_1 > \frac{1}{4}$,

$$v_{(-)}(p, \mathbf{k}_{0j}) = 2^{-1/2}(1, -1) \tag{16b}$$

at $\mathbf{k}_{0j} = (100), (010), (001)$.

There is only one possible density distribution that yields the stoichiometric composition $c = c_{st} = \frac{3}{4}$ within the range of interaction energies providing the eigenvector (16*a*). This is

$$\begin{aligned} n(p, \mathbf{R}) = c + \eta[&\gamma_{(-)}(\mathbf{k}_{100})v_{(-)}(p, \mathbf{k}_{100}) \exp(i2\pi\mathbf{k}_{100}\mathbf{R}) \\ &+ \gamma_{(-)}(\mathbf{k}_{010})v_{(-)}(p, \mathbf{k}_{010}) \exp(i2\pi\mathbf{k}_{010}\mathbf{R}) \\ &+ \gamma_{(-)}(\mathbf{k}_{001})v(p, \mathbf{k}_{001}) \exp(i2\pi\mathbf{k}_{001}\mathbf{R})]. \end{aligned} \tag{17}$$

At $c = c_{st} = \frac{3}{4}$ and $\gamma_{(-)}(\mathbf{k}_{100}) = \gamma_{(-)}(\mathbf{k}_{010}) = \gamma_{(-)}(\mathbf{k}_{001}) = -2^{-3/2}$, (17) may be written in the form

$$n(p, \mathbf{R}) = n(p, x, y, z) = \begin{cases} \frac{3}{4} - (\eta/4)[\exp(i2\pi x) \\ \quad + \exp(i2\pi y) \\ \quad + \exp(i2\pi z)], \ p = 1 \\ \frac{3}{4} - (\eta/4)[\exp(i2\pi x) \\ \quad + \exp(i2\pi y) \\ \quad + \exp(i2\pi z)], \ p = 2, \end{cases} \tag{18}$$

where $\mathbf{R} = x\mathbf{a}_1 + y\mathbf{a}_2 + z\mathbf{a}_3$, (x, y, z) are coordinates of a site of the f.c.c. lattice, $\mathbf{k}_{100}\mathbf{R} = x$, $\mathbf{k}_{010}\mathbf{R} = y$, $\mathbf{k}_{001}\mathbf{R} = z$. At $\eta = 1$ the distribution (18) assumes only two values, 1 and 0. If oxygen atoms are placed into the interstices at which $n(p, \mathbf{R}) = 1$ and vacancies into the interstices at which $n(p, \mathbf{R}) = 0$, the structure depicted in Fig. 1 is produced. This simple cubic structure is related to the fluorite structure but has ordered oxygen vacancies in the $\langle 111 \rangle$ directions.

The situation is more complicated within the energy range related to the eigenvector (16*b*). In this case, a distribution function generated by the eigenvectors (16*b*) and describing a completely ordered state with stoichiometric composition $c_{st} = \frac{3}{4}$ cannot be constructed. The only option is the choice of the distribution function in the following form:

$$\begin{aligned} n(p, \mathbf{R}) = c + \eta_1[&\gamma_{(-)}(\mathbf{k}_{100})v_{(-)}(p, \mathbf{k}_{100}) \exp(i2\pi\mathbf{k}_{100}\mathbf{R}) \\ &+ \gamma_{(-)}(\mathbf{k}_{010})v_{(-)}(p, \mathbf{k}_{010}) \exp(i2\pi\mathbf{k}_{010}\mathbf{R})] \\ &+ \eta_2\gamma_{(+)}(\mathbf{k}_{001})v_{(+)}(p, \mathbf{k}_{001}) \exp(i2\pi\mathbf{k}_{001}\mathbf{R}), \end{aligned} \tag{19}$$

in which an additional wave $\omega_{(+)}(p, \mathbf{k}_{001}) = 2^{-1/2}(1, 1) \exp(i2\pi\mathbf{k}_{001}\mathbf{R})$, corresponding to the higher eigenvalue, $\lambda_{(+)}(\mathbf{k}_{001})$, has to be included. Therefore, we have to introduce two long-range parameters that change with temperature in different ways.

At $c = c_{st} = \frac{3}{4}$ and $\gamma_{(-)}(\mathbf{k}_{100}) = \gamma_{(-)}(\mathbf{k}_{010}) = \gamma_{(+)}(\mathbf{k}_{001}) = -2^{-3/2}$, (18) has the form

$$n(p, \mathbf{R}) = n(p, x, y, z) = \begin{cases} \frac{3}{4} - (\eta/4)[\exp(i2\pi x) \\ \quad + \exp(i2\pi y)] - (\eta_2/4) \\ \quad \times \exp(i2\pi z) \text{ for } p = 1 \\ \frac{3}{4} + (\eta_1/4)[\exp(i2\pi x) \\ \quad + \exp(i2\pi y)] - (\eta_2/4) \\ \quad \times \exp(i2\pi z) \text{ for } p = 2. \end{cases} \tag{20}$$

For the fully ordered state ($\eta_1 = \eta_2 = 1$), (20) may be rewritten as

$$n(p, \mathbf{R}) = \begin{cases} \frac{3}{4} - \frac{1}{4}[\exp(i2\pi x) + \exp(i2\pi y) \\ \quad + \exp(i2\pi z)] \text{ for } p = 1 \\ \frac{3}{4} - \frac{1}{4}[-\exp(i2\pi x) - \exp(i2\pi y) \\ \quad + \exp(i2\pi z)] \text{ for } p = 2 \end{cases} \tag{21}$$

and assumes only two values 0 and 1 on all tetrahedral interstices. Placing O atoms into interstices at which $n(p, \mathbf{R}) = 1$ and vacancies into interstices at which $n(p, \mathbf{R}) = 0$ yields the structure depicted in Fig. 2. This structure is tetragonal and is characterized by rows of vacancies aligned along the c axis. Its symmetry is determined by the space group $P4_2/mcm$. It follows from Fig. 2 that the O atoms are situated in two non-equivalent positions. The atoms that are nearest neighbours of vacancies will be called O_I, while the atoms surrounded only by other oxygen atoms will be called O_{II}.

3. Comparison with observed results

The assumed disordered state for high-temperature Bi_2O_3 is in agreement with X-ray powder diffraction data (Gattow & Schröder, 1962). Gattow & Schröder proposed a model of δ-Bi_2O_3 with the f.c.c bismuth host structure, 3/4 of its tetrahedral sites being randomly occupied by O atoms. This structure was also confirmed by the neutron diffraction data for Bi_2O_3 at 1047 K (Harwig, 1978). It has, however, been shown in this paper that the best fit between observed and calculated intensities is attained if, following the Willis model (Willis, 1963, 1964, 1965), each oxygen atom in a tetrahedral site is replaced by four 'quarter O atoms' displaced from the position xxx, $x = \frac{1}{4}$ to xxx, $x = \frac{1}{4} + u$. This observation, in fact, demonstrates strong anisotropic thermal-motion-induced delocalization of oxygen atoms about tetrahedral sites and thus does not contradict the tetrahedral occupancy model. Indeed, one can readily see that the superposition of four spherical or ellipsoidal Gaussian distributions (spherical or ellipsoidal distributions follow from the Debye–Waller harmonic approximation for thermal vibrations), displaced according to the Willis model from a tetrahedral site to the nearest octahedral sites by the distance $u3^{1/2}$, approximates the anisotropic oxygen distribution stretched out to these octahedral sites.

The abnormally large value of the observed temperature factors for the oxygen atoms [$B_O = 24{\cdot}6$ Å^2, whereas $B_{Bi} = 3{\cdot}5$ Å^2 (Harwig, 1978)] is further confirmation of strong thermal delocalization of oxygen atoms. The considerable stretching of the oxygen distribution from a tetrahedral interstice to the nearest octahedral interstices and the observed superionic conductivity in δ-Bi_2O_3 (Takahashi, Iwahara & Nagai, 1972; Takahashi & Iwahara, 1973; Takahashi, Iwahara & Arao, 1975; Takahashi, Esaka & Iwahara, 1975, 1976, 1977), caused by a small diffusion barrier for O atoms, seem to be related phenomena.

A different structure for δ-Bi_2O_3 was proposed by Sillen (1937), who used X-ray powder diffraction data. The Sillen model, unlike the model offered by Gattow & Schröder, has an ordered distribution of O atoms and is in complete agreement with the structure predicted in § 2 and presented in Fig. 1.

Since X-ray intensity measurements are not sufficiently sensitive to O-atom positions, they cannot successfully distinguish between the two models. Because of this, the electron diffraction study, which revealed superlattice reflections in the diffraction pattern of δ-Bi_2O_3, is of special interest (Zavyalova & Imamov, 1969). Observation of the extra diffraction spots related to the star {100} of the f.c.c. parent enabled the authors to arrive at the conclusion that the observed δ phase has the structure that coincides with that proposed by Sillen and thus agrees with the model presented in Fig. 1. At the same time, a neutron diffraction study (Harwig, 1978) failed to reveal the superlattice reflection from δ-Bi_2O_3 and this led to the conclusion that the δ phase is a disordered phase described by the Gattow–Schröder model.

This controversy can be resolved if we assume that the various authors regarded both phases, ordered and disordered, as the same δ phase. It should be noticed that both phases are predicted by the theory presented in § 2.

The structure of the β-Bi_2O_3 phase was determined from single-crystal X-ray and neutron powder diffraction data (Aurivillius & Malmros, 1972). By carefully

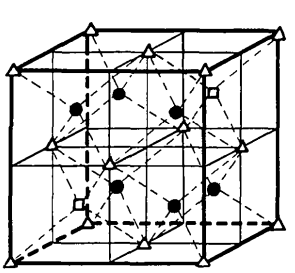

Fig. 1. Theoretically predicted structure of the ordered δ phase. Oxygen vacancies are ordered in ⟨111⟩ directions. □ Oxygen vacancy; ● oxygen atoms; △ bismuth atoms.

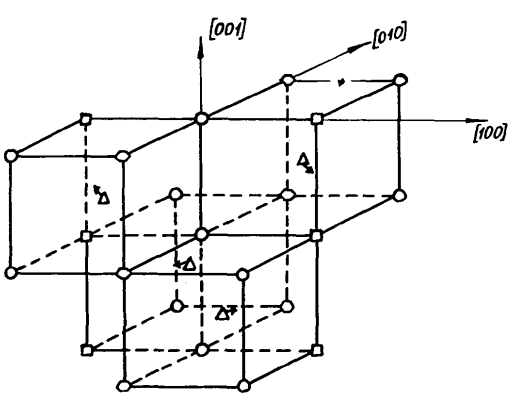

Fig. 2. Structure of the virtual β_0 phase (space group $P4_2/mcm$) as predicted by the concentration-wave method. Shifts of Bi atoms toward rows of vacancies are depicted by arrows. Here and in other figures: □ oxygen vacancy; ○ oxygen-atom nearest neighbours of vacancies (O_I); ◯ oxygen-atom next-nearest neighbours of vacancies (O_{II}); △ bismuth atom.

observing the structure of the β phase ($P\bar{4}2_1c$) proposed by Aurivillius & Malmros, one may recognize that it would fit the theoretically predicted structure depicted in Fig. 2, if the shifts from the ideal crystallographic positions were assumed to be zero. The shifts reduce the space-group symmetry of the ordered phase in Fig. 2 to $P\bar{4}2_1c$ and account for the observed $\{\frac{1}{2}\frac{1}{2}0\}$-type extra superlattice reflections. Displacements reducing the symmetry of a phase cannot be explained by the conventional static theory as displacements caused by an ordered distribution of oxygen vacancies within the Bi host lattice. Thus, we arrive at the conclusion that in the β phase we deal with the situation mentioned in the *Introduction*, which is more complicated than mere atomic ordering. In this case, a displacive transformation resulting in a reduction of the symmetry is imposed on the ordering of oxygen vacancies in the fluorite-type structure. The microscopic nature of this transformation is interesting enough to deserve extensive discussion.

The connection of distortion in bismuth oxides to electronic configuration was recognized earlier (Orgel, 1959; Abrahams, Jamieson & Bernstein, 1967). This idea is developed in the next sections where the specific electron mechanism based on the pseudo-Jahn–Teller effect is utilized (Bersuker, 1966; Vekhter & Bersuker, 1973). This mechanism enables us to determine the displacive mode transforming the parent virtual phase derived in § 2 (it is called hereafter the β_0 phase) into the β phase and thus predict theoretically the structure changes at the transformation.

4. Distortion caused by pseudo-Jahn–Teller effect in the β phase

The outer electron shell of a bismuth atom has the configuration $6s^26p^3$. In chemical compounds its three p electrons can form covalent bonds with other atoms, whereas the two s electrons are the inert electron pair. In Bi and other elements of Group V*b*, P, As, Sb, the vacant d states are known to be involved in covalent bond formation. This effect increases with atomic weight among the elements of Group V*b* and it is the greatest for Bi. The sixfold coordination of a Bi atom in the virtual β_0 phase requires two vacant d states to be involved.

Let us assume that β-Bi_2O_3 is a narrow band oxide. The first approximation for the electron band structure of the β phase can be obtained by analysing the coordination polyhedron of a Bi atom in the virtual β_0 phase as a pseudo molecule. This approximation is reasonably good if the distance between the electron levels in this pseudo molecule is considerably greater than the bandwidth caused by broadening of these levels due to electron tunnelling between nearest coordination polyhedra.

In the β_0-Bi_2O_3 structure each oxygen atom should form two covalent σ bonds with the nearest four Bi atoms. Therefore, two of the valence electrons of a Bi atom form bonds with O_I atoms and the remaining one valence electron forms a bond with O_{II}.

The coordination polyhedron of a Bi atom in the β_0 phase is depicted in Fig. 3(*a*) (compare with Fig. 2). Its point group is C_{2v}. There are two Bi-O_{II} bonding orbitals. One is symmetric about the $(001)_t$ plane drawn through the Bi atom.* It transforms according to the identity irreducible representation A_1 of the point group C_{2v}. The other is antisymmetric about the $(001)_t$ plane and symmetric about the $(010)_t$ plane. This transforms according to the irreducible representation B_1. As usual, let us assume that the state that transforms according to the identity representation A_1 has the lowest energy. We also assume that the energy of the A_1 valence state is $E_0-\Delta$ and that the energy of the B_1 valence state is $E_0+\Delta$, where $\Delta>0$. The valence electron should couple with the displacive mode transforming according to the irreducible representation $A_1\times B_1=B_1$.

If the electron–phonon interaction is taken into account, off-diagonal terms occur in the Hamiltonian,

*The unit cell of the tetragonal β phase with $a_t\simeq a_{f.c.c.}2^{1/2}$, $c_t\simeq a_{f.c.c.}$ is used. The corresponding orientational relations are $[100]_t\|[110]$, $[010]_t\|[1\bar{1}0]$, $[001]_t\|[001]$, where index t is related to the tetragonal phase.

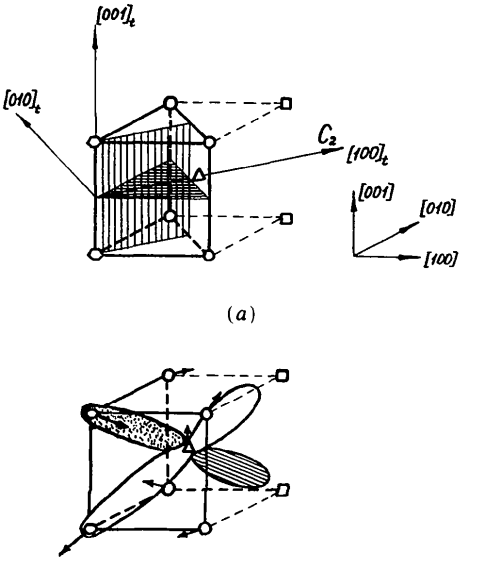

Fig. 3. Coordination polyhedron of Bi atom in the virtual β_0 phase. (*a*) Symmetry elements. Here and in other figures the coordinate axes $[100]_t\|[110]$, $[010]_t\|[1\bar{1}0]$ and $[001]_t\|[001]$ are used. The symmetry planes are hatched. C_2 is the twofold axis. The coordinate system used previously is depicted on the right for comparison. (*b*) Shifts and alignment of orbitals at the phase transition in the coordination polyhedron. Here and in other figures the filled valence orbital is, dotted, the filled inert-pair orbital is hatched.

which for the relevant case has the form

$$H_{ij}=\begin{pmatrix} E_0-\Delta+(m\omega^2/2)Q^2 & VQ \\ VQ & E_0+\Delta+(m\omega^2/2)Q^2 \end{pmatrix}, \quad (22)$$

where $i, j=1$ for the A_1 state and $i,j=2$ for the B_1 state; Q is the amplitude of the displacive mode which transforms according to the B_1 irreducible representation (collective coordinate), V is the electron-phonon coupling constant, $(m\omega^2/2)Q^2$ is the elastic energy increase caused by displacement Q, ω is the B_1 phonon mode frequency and m is close to oxygen atomic mass m_O, since $m_O/m_{Bi} \ll 1$ (Opik & Pryce, 1957).

The eigenvalue of the Hamiltonian (22) is

$$E_t(Q)=E_0+(m\omega^2/2)Q^2 \pm (\Delta^2+V^2Q^2)^{1/2}. \quad (23)$$

If the electron-phonon coupling constant V is large enough so that

$$V(m\omega^2\Delta)^{-1/2}>1, \quad (24)$$

the energy $E_-(Q)$ no longer assumes the minimum value at $Q=0$, but is attained at

$$Q=Q_0=\pm[(V/m\omega^2)^2-(\Delta/V)^2]^{1/2}. \quad (25)$$

Thus a first-order phase transition, often called the pseudo-Jahn-Teller effect, occurs. The superionic conductivity of disordered Bi_2O_3 (Takahashi *et al.*, 1972; Takahashi & Iwahara, 1973; Takahashi, Iwahara & Arao, 1975; Takahashi, Esaka & Iwahara, 1975, 1976, 1977) and its huge temperature factor (Harwig, 1978) imply an abnormally low value of $m\omega^2$ (according to the Debye-Waller theory the temperature factor is proportional to $B \sim k_BT/m\omega^2$) and that favours the pseudo-Jahn-Teller transition.

Criterion (24) is valid for $T=0$ when the entropy contribution to the free energy vanishes. At $T \neq 0$, criterion (24) can readily be modified by taking into account the equilibrium electron occupancy of both E_- and E_+ levels.

The eigenvector of the Hamiltonian (22) is

$$\begin{aligned}\alpha_\pm(p)&=[\alpha_\pm(1), \alpha_\pm(2)]\\ &=[1+\{\Delta/VQ\pm[(\Delta/VQ)^2+1]^{1/2}\}^2]^{-1/2}\\ &\quad\times\{1, \Delta/VQ\pm[(\Delta/VQ)^2+1]^{1/2}\}. \end{aligned} \quad (26)$$

These eigenvectors are related to the wavefunctions

$$\begin{aligned}\varphi_\pm&=\alpha_\pm(1)\varphi_{A_1}+\alpha_\pm(2)\varphi_{B_1}\\ &=[1+\{\Delta/VQ_0\pm[(\Delta/VQ_0)^2+1]^{1/2}\}^2]^{-1/2}\\ &\quad\times[\varphi_{A_1}+\{\Delta/VQ_0\pm[(\Delta/VQ_0)^2+1]^{1/2}\}\varphi_{B_1}], \end{aligned} \quad (27)$$

where φ_{A_1} is the fully symmetric wavefunction, and φ_{B_1} is the wavefunction of the state antisymmetric about the plane $(001)_t$. In the extreme case $\Delta/VQ_0 \ll 1$ [one may easily see that this condition amounts to the stronger inequality (24), *i.e.* $V(m\omega^2\Delta)^{-1/2} \gg 1$], we have

$$\alpha_\pm(p) \to 2^{-1/2}(1, \pm 1) \quad (28)$$

and

$$\varphi_\pm=2^{-1/2}(\varphi_{A_1}\pm\varphi_{B_1}). \quad (29)$$

It should be mentioned that the strong inequality assumed above is not really necessary for further consideration. It just simplifies all the conclusions and makes them more obvious. The wavefunctions φ_+ describe valence orbitals that point only at one of the two O_{II} atoms (Fig. 3*b*). As a result of the phase transition, the φ_- state corresponding to the lower eigenvalue E_- is filled by the valence electron and the φ_+ state is empty (Fig. 3*b*). In this case the covalent bond is formed with one of the two O_{II} atoms, making the distance between Bi and this O_{II} atom shorter than that between Bi and the other O_{II} atom.

The same consideration can be applied to the inert electron pair of the Bi atom at the centre of the coordination polyhedron in the β_0 virtual phase. The inert pair is affected by the electric field of the ligands of the same symmetry as the field that affects the valence electron involved in bond formation with two O_{II} atoms. Therefore, the inert electron-pair orbitals should also transform according to the same irreducible representations A_1 and B_1 as the valence electron orbitals. Since two oxygen vacancies of the coordination polyhedron can be regarded as positive charges, their field affects the inert pair in such a way that the wavefunction of the inert pair points to the vacancies. Therefore, the inert electrons couple with the displacive mode transforming according to the irreducible representation B_1 as well as to the valence electron. Thus the interaction of the inert pair with the displacive mode B_1 yields an additional contribution to the driving force of the displacive transformation.

The valence electron and the inert pair are more removed from each other and the repulsion electrostatic energy is lower if their orbitals are aligned along the same body diagonal. Therefore, we are able to conclude that the inert electron pointing at the vacancy and the valence orbital pointing at the O_{II} atom (it provides the Bi-O_{II} bond) are aligned along the same body diagonal of the coordination polyhedron.

Let us assume the high-symmetry β_0 phase to be the reference state. Transition of the valence electron and the inert pair at the pseudo-Jahn-Teller transition on one of the body diagonals amounts to addition of the negative charge to the filled shadowed and hatched orbitals and addition of the positive charge to the empty orbitals (see Fig. 3*b*). This electron redistribution produces an O_{II}-atom shift toward the Bi atom along its Bi-O_{II} bond (along the shadowed orbital) and the other O_{II} atom moves along the direction of the empty orbital away from the Bi atom.

Four O_I atoms shift approximately along the additional electric field at their positions caused by the electron redistribution. The resulting shifts of O atoms in a coordination polyhedron are depicted in Fig. 3(*b*).

Since the crystal is formed by packing coordination polyhedra, the pseudo-Jahn–Teller transitions in the polyhedra cannot occur independently. The electron–phonon interaction yields the interaction between directions of filled orbitals in different coordination polyhedra and thus results in the cooperative pseudo-Jahn–Teller transition.

The maximal point symmetry of a portion of the structure of the β_0 phase is D_{2d}. The minimal portion with D_{2d} symmetry consists of the four nearest coordination polyhedra sharing oxygen vacancies. Let us call it a complex. Such a complex will be considered below in order to determine mutual alignment of orbitals in the nearest polyhedra (Fig. 4).

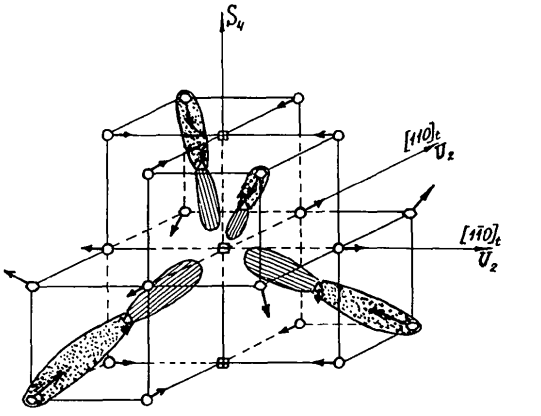

(*a*)

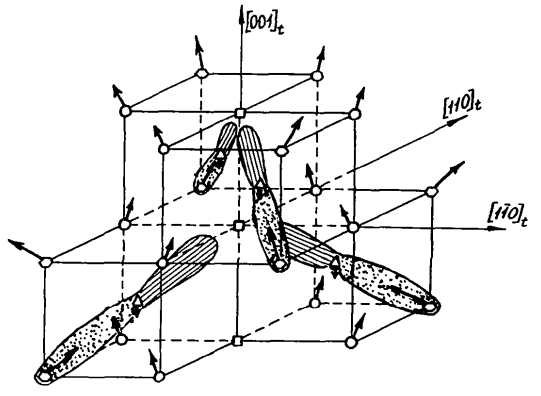

(*b*)

Fig. 4. Distortion and orbital alignment at the phase transition in the complex of symmetry D_{2d} of four coordination polyhedra (*a*) induced by the identity representation a_1; (*b*) induced by the irreducible representation b_2. Here and in other figures: ⊞ 'plus' vacancy; ⊟ 'minus' vacancy. U_2 are the horizontal twofold axes. S_4 is the fourfold rotoflection axis.

The displacive modes of the complex, as well as the directions of orbitals at the phase transformation, should have the symmetry of one of the irreducible representations of the D_{2d} group. Expansion of the mechanical reducible representation of atomic displacements in irreducible representations of the D_{2d} group yields the identity representation a_1, the one-dimensional irreducible representation b_2 and the two-dimensional irreducible representation e.

Displacements transforming according to the e representation are zero for two polyhedra of the complex and thus cannot yield the maximum energy gain at the phase transformation. This is the reason why this option should be rejected.

The distortion and filled orbital directions transforming according to the irreducible representation b_2 are depicted in Fig. 4(*b*). If the crystal is packed with such complexes, the phase transformation yields a ferroelectric phase.

Displacements and orbital directions transforming according to the identity representation a_1 are depicted in Fig. 4(*a*). It is shown below that such displacements produce an antiferroelectric transition.

The symmetry analysis carried out above reduces the choice between various displacement modes that might be responsible for the pseudo-Jahn–Teller transformation to two. The final choice could be made if we knew the values of the electron–phonon coupling constant V and frequency ω for each of two modes, a_1 and b_2. The phase transformation is generated by the mode that provides the lower value E_- [see (23)]. Unfortunately, the available information on the dynamical properties of the system is not sufficient to allow a choice between the two modes. But a certain qualitative consideration in favour of the identity a_1 mode, resulting in the antiferroelectric phase, can be made. It follows from Fig. 4(*a*) that the axes $[110]_t$ and $[1\bar{1}0]_t$ drawn through the central vacancy are the twofold axes U_2 of the complex, and the displacements of O_I atoms thus are along the directions $[110]_t$ and $[1\bar{1}0]_t$ to the nearest vacancies of the neighbouring complexes. This is not the case for the ferroelectric phase composed of complexes depicted in Fig. 4(*b*). With this difference between the complexes in Fig. 4 taken into account, it is natural to assume that the structure in which atoms shift toward vacancies is more stable than that in which atoms shift in a different direction. Proceeding from this conclusion we shall determine the crystal structure of the anti-ferroelectric phase composed of distorted complexes depicted in Fig. 4(*a*).

Let us call vacancies at which four filled orbitals point 'plus' vacancies and vacancies at which no filled orbitals point 'minus' vacancies (see Fig. 4*a*). This drives us to the unambiguous conclusion that plus and minus vacancies alternate along the tetragonal axis $[001]_t$. Let us consider how complexes such as those depicted in Fig. 4(*a*) may be packed in the β_0

phase unit cell. It follows from Fig. 2 that each O_I atom has two nearest-neighbour vacancies. If those vacancies were of the same sort, their effect on the O_I atom would cancel, *i.e.* this O_I atom would not displace and thus would not contribute to the driving force of the pseudo-Jahn–Teller transition. The only other option is that the two vacancies nearest to an O_I atom are of a different sort. Therefore, minus and plus vacancies should alternate along the $[110]_t$ and $[0\bar{1}0]_t$ axes drawn through the vacancies as well as along the $[001]_t$ direction. Since mutual location of plus and minus vacancies and, consequently, directions of filled orbitals are determined, the space group of the phase formed from the β_0 phase due to the pseudo-Jahn–Teller effect (we shall call it the β_1 phase) can be unambiguously determined. The atomic shifts shown in Fig. 5 reduce the symmetry $P4_2/mcm$ of the virtual β_0 phase to the symmetry $P4_2/nmc$ (No. 137) of the β_1 phase, which is, however, still higher than the symmetry of the space group $P\bar{4}2_1c$ observed for the β phase (Aurivillius & Malmros, 1972). The structures of β_1 and β phases are close to each other, but the group $P4_2/nmc$ obtained theoretically has extra twofold axes $[110]_t$ and $[1\bar{1}0]_t$ passing through O_I atoms and vacancies and extra reflection planes $(100)_t$ and $(010)_t$ drawn through rows of vacancies and O_{II} atoms along the $[001]_t$ axis. The latter in fact means that the structure of the experimentally observed β phase can be obtained from the structure of the β_1 phase if the mechanism is found for the displacive mode [antisymmetric about the additional reflection planes, $(100)_t$ and $(010)_t$] that removes these symmetry elements (see Fig. 4*a*).

The key fact that enables one to understand the nature of the transition is the following. According to the observed results the β phase exists only in an atmosphere poor in oxygen, *i.e.* the β phase is more stable when it contains less O atoms than required by the stoichiometric formula Bi_2O_3 (Fomchenkov, Mayer & Gracheva, 1974). This result is in agreement with the X-ray data showing that the composition of the observed β phase is described by the formula $Bi_2O_{2.5}$ (Zavyalova & Imamov, 1971). Therefore, the β phase is stabilized by an additional number of vacancies, which affect the electronic structure of β-Bi_2O_3. Indeed, at the stoichiometric composition, electrons completely occupy both Bi–O_I bonding states, G and U, which are symmetric and antisymmetric about the $(010)_t$ plane, respectively (Fig. 3*a*). These states couple with the displacive mode, transforming according to an irreducible representation antisymmetric about the $(010)_t$ planes, since $G \times U = U$. Shifts of G and U levels (23) caused by antisymmetric distortion do not affect the overall electron energy, because a decrease in energy of the lower completely occupied G level is exactly compensated for by an increase in energy of the completely occupied higher U level. This is not the case for the non-stoichiometric β phase in which O_I atom vacancies are formed. Vacancy formation results in a situation where the higher antisymmetric Bi–O_I bonding level U, unlike the lower bonding level G, is occupied only partially. In this case, the decrease in energy of the completely occupied lower G level caused by distortion is not compensated for by increase in energy of the partially occupied higher U level, *i.e.* the total energy of the system decreases. This means that the virtual β_1 phase is unstable against displacements of O_I and Bi atoms antisymmetric about the $(010)_t$ plane. In other words, the displacive transformation of the β_1 phase removes the symmetry about the $(010)_t$ plane.

According to (27), electron density providing Bi–O_I bonding in the β_1 phase is mainly concentrated between the Bi atom and those O_I atoms of its coordination polyhedron (neighbours of the plus vacancy)

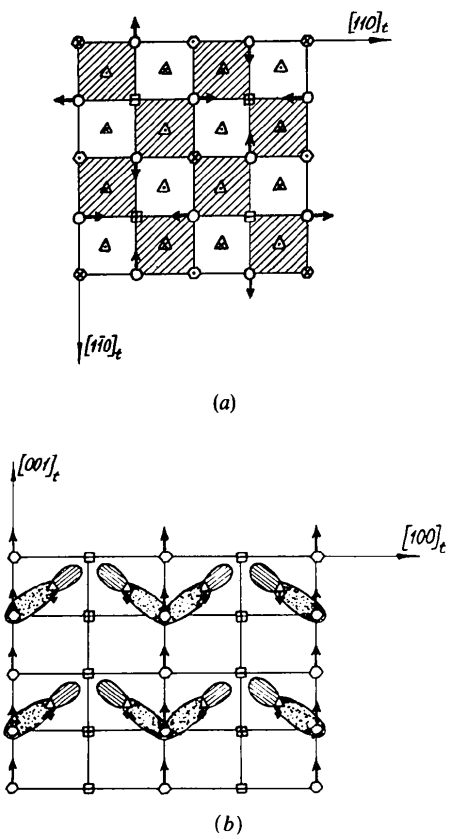

Fig. 5. Theoretically obtained first displacive phase transition ($P4_2/mcm \rightarrow P4_2/nmc$). Here and in other figures: ⊙ △ ⊙, *i.e.* a point in the middle of sign of an atom, denotes shift toward positive z, ⊗ ▲ ⊗, *i.e.* a cross in the middle of sign of an atom, denotes shift toward negative z. (*a*) Projection of the structure obtained on the plane $(001)_t$ drawn through vacancies and O_I atoms. Here and in other figures Bi atoms in hatched squares are above the plane of projection (positive z); Bi atoms in non-hatched squares are below the plane of projection (negative z). (*b*) Cross section of the plane $(010)_t$ drawn through vacancies and O_{II} atoms.

that shift toward the vacancy, whereas the bonding electron density between the Bi atom and those O_I atoms of its coordination polyhedron (the neighbours of the minus vacancy) that shift from the vacancy is much smaller. This is the reason why a distortion inducing the relevant secondary displacive transformation should be chosen so that the maximum length difference of two Bi-O_I bonds with O_I atoms on both sides of the $(010)_t$ plane neighbouring the plus vacancy is ensured. Such a choice provides the maximum gap between the valence Bi-O_I levels.

As before, let us examine a complex of the D_{2d} point group of four coordination polyhedra sharing vacancies (see Fig. 4*a*). It was shown above that coordination polyhedra are unstable against a displacive mode antisymmetric about the $(010)_t$ plane. This result, when applied to the complex of four polyhedra depicted in Fig. 4(*a*), means that the complex is unstable against the displacive mode antisymmetric about the $(100)_t$ and $(010)_t$ planes. In terms of point-group theory, this phase-transition instability is caused by the displacive mode transforming according to an irreducible representation of the point group D_{2d} whose character $\chi(\hat{\sigma}_D)$ is equal to -1, where $\hat{\sigma}_D$ are reflections about the $(100)_t$ and $(010)_t$ planes. There are only two irreducible representations such that $\chi(\hat{\sigma}_D)=-1$. They are one-dimensional representations a_2 and b_1. Displacements transforming according to these irreducible representations are depicted in Figs. 6(*a*) and 6(*b*).

The shifts of O_I atoms transforming according to the b_1 irreducible representation are in the directions $\langle 11.0\rangle_t$, *i.e.* $\pm[110]_t$ and $\pm[1\bar{1}0]_t$, whereas the shifts of O_I atoms transforming according to the a_2 representation should be in directions perpendicular to the $\langle 11.0\rangle_t$. The directions of O_I shifts should be as close to the Bi-O_I bond directions (which are the body-diagonal directions $\langle 10.1\rangle_t$ of the coordination polyhedra, if the effect of Bi shifts is not taken into account) as possible to ensure the greatest possible change in Bi-O_I bond lengths and thus the greatest possible energy gain at the phase transformations. The latter conclusion and the requirement that O_I shifts should be along directions normal to $\langle 11.0\rangle_t$ yield the $\langle 11.2\rangle_t$ directions of O_I shifts for the a_2 irreducible representation. The directions $\langle 11.2\rangle_t$ obtained in this way are closer to the Bi-O_I bond directions (which are approximately the $\langle 10.1\rangle_t$ directions) than the $\langle 11.0\rangle_t$ directions of the O_I shifts transforming according to the irreducible representation b_1. Therefore, the a_2 irreducible representation of the D_{2d} point group should be singled out as the one that provides the greatest energy gain and thus induces the second phase transformation.

All four O_I atoms depicted in Fig. 6(*a*) rotate about the axis $[001]_t$ drawn through the vacancy. At the same time, the component along the $[001]_t$ axis of the displacements of the nearest O_I atoms in the $(001)_t$ plane are of opposite sign. The $[001]_t$ axes drawn through the rows of vacancies are no longer screw axes, as would be required in the space group $P4_2/nmc$ of the β_1 phase, but turn into $\bar{4}$ axes. As for the Bi atoms, they should rotate in the opposite direction to the O_I atoms in order to contribute to the difference between Bi-O_I covalent bond lengths and consequently to the driving force of the displacive transition.

In the nearest-neighbour complexes (see Fig. 6*c*), the rotation directions of the O_I atoms around the respective axes $[001]_t$ should be opposite (if rotation in a complex is clockwise, then rotation in the nearest complex is counterclockwise) so that the displacements should add rather than subtract. Projection of the resulting atomic pattern on the $(001)_t$ plane is presented in Fig. 6(*c*).

Displacements of atoms in the neighbouring $(001)_t$ planes drawn through the vacancies (see Fig. 4*a*) are not interrelated by the symmetry operations of the

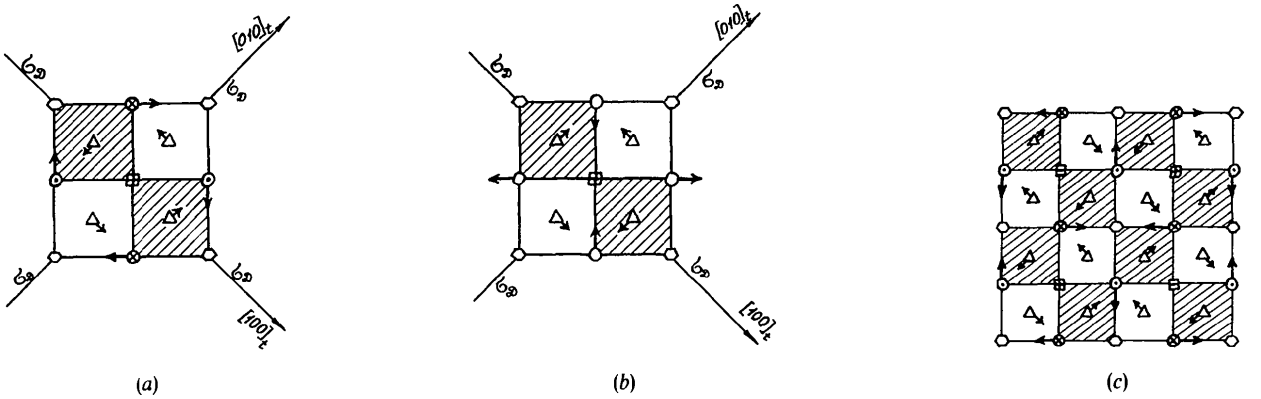

(*a*) (*b*) (*c*)

Fig. 6. Projection on the plane $(001)_t$ drawn through vacancies and O_I atoms of (*a*) distortion in the complex of symmetry D_{2d} of four coordination polyhedra induced by the irreducible representation a_2; (*b*) distortion in the complex of symmetry D_{2d} of four coordination polyhedra induced by the irreducible representation b_1; (*c*) theoretically obtained distortion inducing the second phase transition ($P4_2/nmc \rightarrow P\bar{4}2_1c$). σ_D are the vertical symmetry planes of the complex of four coordination polyhedra.

D_{2d} point group, so that the point-group elements do not impose any constraints on displacements of atoms in the neighbouring $(001)_t$ layers passing through the vacancies. As any $(001)_t$ plane should be a rotoflection plane of the structure of the β phase (see Fig. 6*a*), the period of the structure along the $[001]_t$ axis should be twice the distance between the $(001)_t$ planes drawn through the neighbouring vacancies, *i.e.* it should remain the same as in the virtual β_1 phase. Therefore, displacements of O_I atoms in the $(001)_t$ planes drawn through neighbouring vacancies should be directed either in the same or in the opposite directions. The latter case should be rejected because

(i) in half of all the coordination polyhedra the Bi shift offsets the impact of the O_I shift on the bond length Bi–O_I;

(ii) unlike the foregoing case, distances between nearest-neighbour O_I atoms are affected. Variations of the nearest-neighbour distances raise O_I–O_I interaction energy for the typical situation of a concave O_I–O_I repulsive potential.

Thus, the displacements of oxygen atoms in the $(001)_t$ planes drawn through neighbouring vacancies should be the same, *i.e.* vertical rows of O_I atoms should displace as a whole.

Thus, a displacive mode inducing a second phase transition $\beta_1 \rightarrow \beta$ is obtained. It does not change the period of the virtual β_1 phase of the crystal structure (it corresponds to the wavevector $\mathbf{k}=0$) and reduces the $P4_2/nmc$ space group of the virtual β_1 phase to $P\bar{4}2_1c$ of the β phase. This structure, obtained theoretically as a result of a secondary displacive transformation, agrees with the structure of the β phase reported by Aurivillius & Malmros (1972).

5. Discussion

The resulting displacements yield the space group $P\bar{4}2_1c$, which completely agrees with the experimental results obtained by Aurivillius & Malmros. The only difference is that the z component of displacements proposed by Aurivillius & Malmros is of opposite sign to the z component of all the displacements obtained above. According to the relevant theory, the O_{II} atoms, which are situated on the same body diagonal as the vacancy from which O_I atoms are repelled, should approach the Bi atom. The model of Aurivillius & Malmros yields the opposite result. This contradiction may be readily resolved if one recognizes that the change $z \rightarrow -z$ for all displacement components does not affect the X-ray reflection intensities. This means that diffraction data obtained for the β phase do not enable one to distinguish between the two models. The latter conclusion shows that the β-Bi_2O_3 structure theoretically predicted in this paper is actually in complete agreement with X-ray diffraction data.

The largest displacements of O atoms correspond to the first $\beta_0 \rightarrow \beta_1$ transition involving one empty band and one completely filled band. Therefore, the energy gain due to the band shifts is comparatively large. The second $\beta_1 \rightarrow \beta$ transition yields much smaller atomic displacements and, consequently, a much smaller energy gain, since one of the bands is not empty but partially filled and the other is completely filled. In reality, only the ultimate β-Bi_2O_3 phase ($P\bar{4}2_1c$) exists, whereas intermediate β_0 and β_1 phases seem to be virtual and have never been observed.

The entire consideration of the two successive displacive transformations was carried out for the tight binding approximation, where electron hopping between the nearest coordination polyhedra is neglected. In the real situation, the electron levels of coordination polyhedra considered above broaden into valence bands, the bandwidths of which depend on the tunnelling between polyhedra and the electron-phonon interaction is determined by the energy gap between two valence bands that originate from the A_1 and B_1 levels rather than by the energy gap, 2Δ, between these levels. The phase transitions caused by interband electron-phonon interaction often occurs, for example, in ferroelectrics with narrow forbidden bands (Bersuker, 1966; Vekhter & Bersuker, 1973; Kristofel & Konsin, 1967, 1968, 1973) and in ferroelectrics with impurity levels within the wide forbidden band (Chanussot, 1974).

The example of the structure determination in Bi_2O_3 demonstrates that the proposed approach could be successfully utilized for theoretical determination of the structure of certain compounds that are formed as a result of the combination of atomic redistributions and displacive transformations. The first part of the structure determination, which may be reduced to the atomic redistribution, can be successfully solved by the method of static concentration waves. As for the displacive transformations, the method we use may be employed to study compounds of heavy atoms with narrow bandwidths or compounds with wide bandwidths doped with impurities.

The heavy metals that have inert electron pairs very often form compounds with very distorted coordination polyhedra around metal atoms (Orgel, 1959). These metals are thallium, mercury, lead, bismuth of the sixth period; tin, indium and antimony of the fifth period and, less often, germanium and arsenic. The extent of distortion increases with atomic weight (Orgel, 1959). This can be easily understood if the electron-phonon interaction is assumed to account for the distortion of coordination polyhedra. Indeed, according to criterion (24) the tendency of a coordination polyhedron to distort increases with decreasing forbidden bandwidth. The difference in energy of different atomic orbital states, which as a matter of

fact determines the forbidden bandwidth, decreases in its turn with atomic number.

This approach may be useful in trying to explain atomic displacements that bring about ferroelectric, antiferroelectric or ferroelastic properties of heavy-metal compounds.

References

ABRAHAMS, S. C., JAMIESON, P. S. & BERNSTEIN, J. L. (1967). *J. Chem. Phys.* **47**, 4034-4041.

AURIVILLIUS, B. & MALMROS, G. (1972). *K. Tek. Hoegsk. Handl.* **291**, 544-562.

BERSUKER, I. B. (1966). *Phys. Lett.* **20**, 589-590.

CHANUSSOT, G. (1974). *Ferroelectrics*, **8**, 671-683.

FOMCHENKOV, L. P., MAYER, A. A. & GRACHEVA, N. A. (1974). *Izv. Akad. Nauk SSSR*, **10**, 2020-2023 (in Russian).

GATTOW, G. & SCHRÖDER, H. (1962). *Z. Anorg. Allg. Chem.* **318**, 176-189.

HARWIG, H. A. (1978). *Z. Anorg. Allg. Chem.* **444**, 151-166.

KHACHATURYAN, A. G. (1962). *Phys. Met. Metallogr. (USSR)*, **13**, 493-501.

KHACHATURYAN, A. G. (1963). *Sov. Phys. Solid State*, **5**, 16-24, 548-555.

KHACHATURYAN, A. G. (1973). *Phys. Status Solidi B*, **60**, 9-37.

KHACHATURYAN, A. G. (1978). *Prog. Mater. Sci.* **22**, 1-150.

KHACHATURYAN, A. G. & POKROVSKII, B. I. (1985). *Prog. Mater. Sci.* **29**, 1-138.

KRISTOFEL, N. & KONSIN, P. (1967). *Phys. Status Solidi*, **21**, K39-K43.

KRISTOFEL, N. & KONSIN, P. (1968). *Phys. Status Solidi*, **28**, 731-739.

KRISTOFEL, N. & KONSIN, P. (1973). *Ferroelectrics*, **6**, 3-12.

OPIK, U. & PRYCE, M. H. L. (1957). *Proc. R. Soc. London Ser. A*, **238**, 425-447.

ORGEL, L. E. (1959). *J. Chem. Soc.* **12**, 3815-3819.

SILLEN, L. G. (1937). *Ark. Kemi Mineral. Geol.* **12A**, 1-15.

TAKAHASHI, T., ESAKA, T. & IWAHARA, H. (1975). *J. Appl. Electrochem.* **5**, 197-202.

TAKAHASHI, T., ESAKA, T. & IWAHARA, H. (1976). *J. Solid State Chem.* **16**, 317-323.

TAKAHASHI, T., ESAKA, T. & IWAHARA, H. (1977). *J. Appl. Electrochem.* **7**, 31-35.

TAKAHASHI, T. & IWAHARA, H. (1973). *J. Appl. Electrochem.* **3**, 65-72.

TAKAHASHI, T., IWAHARA, H. & ARAO, T. (1975). *J. Appl. Electrochem.* **5**, 187-195.

TAKAHASHI, T., IWAHARA, H. & NAGAI, Y. (1972). *J. Appl. Electrochem.* **2**, 97-104.

VEKHTER, B. G. & BERSUKER, I. B. (1973). *Ferroelectrics*, **6**, 13-14.

WILLIS, B. T. M. (1963). *Proc. R. Soc. London Ser. A*, **274**, 134-144.

WILLIS, B. T. M. (1964). *J. Phys. Radium*, **25**, 431-439.

WILLIS, B. T. M. (1965). *Acta Cryst.* **18**, 75-76.

ZAVYALOVA, A. A. & IMAMOV, R. M. (1969). *Sov. Phys. Crystallogr.* **14**, 331-334.

ZAVYALOVA, A. A. & IMAMOV, R. M. (1971). *Sov. Phys. Crystallogr.* **16**, 516-519.

Acta Cryst. (1986). B**42**, 224-229

Electron-Beam Damage Observed in the Fast Proton Conductor Ammonium/Hydronium β''-Alumina:* a High-Resolution Electron Microscope (HREM) Study†

BY A. K. PETFORD

Center for Solid State Science, Arizona State University, Tempe, Arizona 85287, *USA*

AND C. J. HUMPHREYS

Department of Metallurgy, University of Liverpool, PO Box 147, *Liverpool, England*

(*Received* 28 *March* 1985; *accepted* 5 *November* 1985)

Abstract

Crystals of ceramic ammonium/hydronium β''-alumina [formula $(NH_4)_{1\cdot67-y}(H_3O)_yMg_{0\cdot67}AL_{10\cdot33}O_{17}\cdot(H_2O)_x$] have been examined in a JEOL 200CX high-resolution electron microscope and high-resolution images obtained of the electron-beam-induced damage. The material is of interest owing to its potential use as a fast proton conductor. Two of the damage modes reported have not previously been seen in the β''-aluminas – secondary proton damage and the formation of small gas bubbles within the material. Mechanisms for these two damage modes are proposed. The other damage mode (loss of the cation-containing planes) is the most common result of electron-beam damage in these materials and the collapse vectors present in ammonium/hydronium β''-alumina are discussed.

The structure of the β-aluminas

The β-aluminas are a family of polyaluminates of which the first to be characterized was sodium β-alumina (Bragg, Gottfried & West, 1931) of formula $Na_2O.11Al_2O_3$. Binary sodium β''-alumina (formula $Na_2O.5Al_2O_3$) was first reported by Théry & Briançon (1962). The hexagonal cell of β-alumina contains two 11 Å thick spinel-like layers, of close-packed aluminium and oxygen atoms, which lie perpendicular to the c axis. The spinel blocks are separated

* IUPAC name: ammonium/oxonium β''-alumina.

† Work carried out in the Department of Metallurgy and Science of Materials, Parks Road, Oxford OX1 3PH, England.

0108-7681/86/030224-06$01.50